Improving Accuracy of Transverse Velocity Measurement with a New Limited Diffraction Beam

Jian-yu Lu, Ph.D.

Department of Physiology and Biophysics, Mayo Clinic and Foundation, Rochester, MN 55905, U.S.A.

Abstract — Limited diffraction beams have a large depth of field and have many potential applications. Previously, we have applied one of these beams called the Bessel beam to improve the measurement of velocity vector (both transverse and axial components) of flow over conventional focused beams. In this paper, a new limited diffraction beam called layered array beam is used to further improve the accuracy of the transverse velocity measurement by producing peaks at the boundaries of Doppler spectrum. Because the new beam can be produced with a linear array, the method can be easily incorporated into a commercial scanner. Theory, simulation, and experiment are studied for the method and the results agree excellently with each other. In addition, applications of the new beam for high frame rate imaging (up to 3750 frames/s at 200 mm depth for biological soft tissues) or for dynamic focusing in both transmit and receive without reducing frame rate are discussed.

I. INTRODUCTION

Limited diffraction beams are first developed by Stratton in 1941 [1]. These beams will not spread as they propagate to an infinite distance. In practice, when produced with a finite aperture, they have a large depth of field. Because of this attractive property, these beams have been studied extensively by many other investigators in optics, acoustics, and electromagnetism [2–21].

Previously, a limited diffraction beam called Bessel beam [2] was applied to improve the measurement of velocity vectors [19] (both transverse and axial components of the velocity [22–25]). In this paper, the study is extended with a new limited diffraction beam called layered array beam [6]. Doppler spectra obtained with this beam for a constant velocity vector have peaks (shoulders with Bessel beams) on their boundaries which can be used to accurately determine the transverse velocity. Moreover, because the new beam can be produced with a linear array [6], the method can be easily incorporated into a commercial scanner. In addition, the new beam can be used for high-frame rate imaging (up to 3750 frames/s at 200 mm depth for biological soft tissues) or to achieve dynamic focusing in both transmit and receive without reducing frame rate with simpler hardware than conventional digital beam formers [11–12].

II. THEORY

In this section, we will derive Doppler spectra produced by a layered array beam [6–8]. The derivation will start from the more familiar X waves [14–15].

A. X Waves and Array Beams

From X waves (see (12) in [14]), one obtain limited diffraction array beams [6–8]. X waves are given by

$$\Phi_{X_n}(\vec{r},t) = e^{in\phi}\int_0^\infty B(k)J_n(kr\sin\zeta) \cdot e^{-k[a_0 - i\cos\zeta(z-c_1 t)]}dk, \quad (1)$$

where $n = 0, 1, 2, ...$, $\vec{r} = (r, \phi, z)$ represents a spatial point in the cylindrical coordinates, t is time, r is radial distance, ϕ is polar angle, z is the axial distance, $c_1 = c/\cos\zeta$ is the phase velocity of X waves, $k = \omega/c$ is the wave number, $\omega = 2\pi f$ is the angular frequency, f is the temporal frequency, c is the speed of sound or light, ζ $(0 \le \zeta < \pi/2)$ is the Axicon angle of X waves (the angle between X branches and a plane perpendicular to the direction of the wave propagation) [14], $J_n(\cdot)$ is the nth-order Bessel function of the first kind, $B(k)$ is any well-behaved function that could represent the transfer function of a practical acoustic transducer or electromagnetic antenna, and a_0 is a constant that determines the fall-off speed of the high-frequency components of X waves.

Summing the X waves in (1) over the index, n, we obtain broadband limited diffraction array beams [6–8,11–12] that remain limited diffraction solutions to the isotropic-homogeneous wave equation

$$\Phi_{Array}(\vec{r},t) = \sum_{n=-\infty}^{\infty} i^n e^{-in\theta}\Phi_{X_n}(r,\phi,z-c_1 t), \quad (2)$$

where $0 \le \theta < 2\pi$ is a free parameter and the subscript "Array" represents "array beams". Because

$$\sum_{n=-\infty}^{\infty} i^n J_n(kr\sin\zeta)e^{in(\phi-\theta)} = e^{i(kr\sin\zeta)\cos(\phi-\theta)}, \quad (3)$$

the array beams can be written by [11–12]

$$\Phi_{Array}(\vec{r},t) = \frac{1}{2\pi}\int_{-\infty}^{\infty} T(k)H(k) \cdot e^{ik_x x + ik_y y + ik_z z}e^{-i\omega t}dk, \quad (4)$$

where

$$\frac{T(k)H(k)}{c}e^{ik_x x+ik_y y+ik_z z}, \tag{5}$$

is the temporal Fourier transform (spectrum) of the array beams, $H(k)$ is the Heaviside step function, $T(k) = 2\pi B(k)e^{-ka_0}$, and

$$\begin{cases} k_x = k\sin\zeta\cos\theta = k_1\cos\theta \\ k_y = k\sin\zeta\sin\theta = k_1\sin\theta \\ k_z = k\cos\zeta = \sqrt{k^2 - k_1^2} \geq 0 \end{cases}, \tag{6}$$

and where $k_1 = \sqrt{k_x^2 + k_y^2} = k\sin\zeta$.

B. Doppler Spectra

Assume that a 3D object, $f(\vec{r})$ (reflection coefficient), is composed of randomly positioned point scatterers embedded in a uniform background of a constant speed of sound, the pulse-echo response of the array beam is given by

$$\begin{aligned} R_{k_x,k_y,k_z}(t) &= \int_V f(\vec{r})[\Phi_{Array}(\vec{r},t) * \Phi_{Array}(\vec{r},t)]d\vec{r} \\ &= \frac{1}{2\pi}\int_{-\infty}^{\infty}\frac{T^2(k)H(k)}{c}\left[\int_V f(\vec{r})e^{i2k_x x+i2k_y y+i2k_z z}d\vec{r}\right] \\ &\quad \cdot e^{-i\omega t}dk, \end{aligned} \tag{7}$$

where "*" represents the convolution with respect to time, V is the volume of the object, and where we have used the fact that the spectrum of the convolution of two functions is equal to the multiplication of the spectra of the functions and have assumed that the imaging system is linear. Notice that the integration over V is a 3D spatial Fourier transform of the object function and the integrand of k multiplied by c is the temporal Fourier transform of the echo signals. With the relationship, (7), the object function, $f(\vec{r})$, can be constructed [11–12].

Eq. (7) contains multiple frequencies and multiple scatterers. For simplicity, in the following derivation only single frequency (assume $\frac{T^2(k)H(k)}{2\pi c^2} = \delta(\omega - \omega_0)$, where $\omega_0 = k_0 c$ and δ is the Dirac-Delta function) and single point scatterer ($f(\vec{r}) = \delta(\vec{r} - \vec{r}_0)$, where $\vec{r}_0$ is the position of the point scatterer) will be considered. In addition, the free parameter, k_y in (4), or θ in (6), is assumed to be zero. With $k_y \equiv 0$, the array beams will not be a function of y and thus can be produced with a 1D linear, instead of 2D array, i.e., [6–8,11–12]

$$\Phi_{Layer}(x,z,t) = \frac{1}{2\pi}\int_{-\infty}^{\infty} T(k)H(k)e^{ik_x x+ik_z z}e^{-i\omega t}dk, \tag{8}$$

where the subscript "Layer" represents "layered array beams" which are so called because the shape of the beam is similar to stacked layers [6]. Because the free parameter, k_x, can be either positive or negative representing leftward or rightward going wave, respectively, Eq. (8) can be modified by summing these two waves and dividing the result by 2 (see Eqs. (12)-(14) in [6])

$$\begin{aligned} &\Phi'_{Layer}(x,z,t) \\ &= \frac{1}{2\pi}\int_{-\infty}^{\infty} T(k)H(k)\cos k_x x e^{ik_z z}e^{-i\omega t}dk. \end{aligned} \tag{9}$$

With the above assumptions and (9), Eq. (7) can be simplified (Eq. (25) in [6])

$$R_{k_x,k_z}(t) = \cos^2 k_x x e^{i2k_z z}e^{-i\omega_0 t}. \tag{10}$$

From (10), Doppler spectrum can be obtained. Assume that a point scatterer is moving in the $x-z$ plane and its position is given by (Eq. (19) in [6])

$$\begin{cases} x = x_0 + vt\sin\alpha \\ z = z_0 + vt\cos\alpha \end{cases}, \tag{11}$$

where (x_0, z_0) is the position of the scatterer at $t = 0$, v is the velocity, and α is the angle between the velocity and the propagation axis of waves (Fig. 1). Substituting (11) into (10) and ignoring the secondary Doppler effects (Doppler effects caused by frequency shift), we obtain [6,19]

$$\begin{aligned} R_{k_x,k_z}(t) &= \cos^2\left[k_x v\sin\alpha\left(t - \frac{-x_0}{v\sin\alpha}\right)\right] \\ &\quad \cdot e^{i(2k_z v\cos\alpha-\omega_0)t}e^{i2k_z z_0}. \end{aligned} \tag{12}$$

With the temporal Fourier transform, we obtain the Doppler spectrum (Eq. (27) in [6])

$$\begin{aligned} \widetilde{R}_{k_x,k_z}(\omega) &= \pi\delta(\omega')e^{i2k_z z_0} + \frac{\pi}{2}[\delta(\omega' + 2k_x v\sin\alpha) \\ &\quad + \delta(\omega' - 2k_x v\sin\alpha)]e^{-i\frac{x_0}{v\sin\alpha}\omega'}e^{i2k_z z_0}, \end{aligned} \tag{13}$$

where

$$\omega' = \omega - (\omega_0 - 2k_z v\cos\alpha). \tag{14}$$

It is seen that (13) consists of 3 spectral lines located at

$$\omega = \omega_c, \tag{15}$$

$$\omega = \omega_c - 2k_x v\sin\alpha, \tag{16}$$

and

$$\omega = \omega_c + 2k_x v\sin\alpha, \tag{17}$$

respectively, where

$$\omega_c = \omega_0 - 2k_z v \cos\alpha \tag{18}$$

is the new central frequency caused by the Doppler effects. From (16) and (17), the bandwidth of the spectrum can be calculated

$$\omega_b = 4k_x v \sin\alpha. \tag{19}$$

With the bandwidth (19) and the new central frequency (18), we obtain both the velocity magnitude and the angle of the velocity [19,22]

$$v = \frac{1}{2}\sqrt{\left(\frac{\omega_b}{2k_x}\right)^2 + \left(\frac{\omega_c - \omega_0}{k_z}\right)^2} \tag{20}$$

and

$$\alpha = \tan^{-1}\left[\frac{-\omega_b k_z}{2k_x(\omega_c - \omega_0)}\right]. \tag{21}$$

For multiple frequencies and/or multiple scatterers moving at different velocities, Eqs. (7) and (9) should be used and the line spectrum will be spread around the central frequency and central velocity (see Figs. 3 and 4).

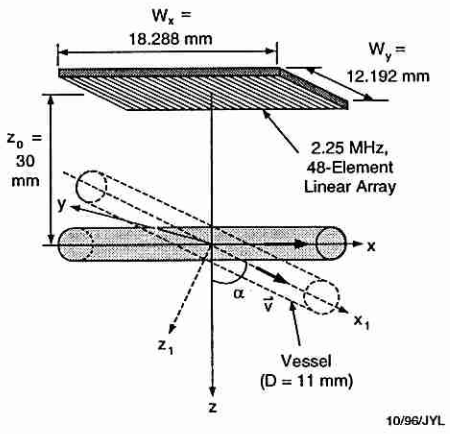

Fig. 1 Geometry for measurement of velocity vectors with a limited diffraction layered array beam produced with a linear array.

III. SIMULATION, EXPERIMENT, AND RESULTS

In this section, computer simulation and experiment for the measurement of velocity vectors will be described and results will be compared with those predicted by theory.

In the simulation, an unfocused, 2.25 MHz, and 48–element linear array transducer was assumed. The dimension of the array was 18.288 mm in the x direction and 12.192 mm in the y (elevation) direction. The free parameter, k_x, in (9) was 1649.13 m^{-1} and the speed of sound c = 1500 m/s. The Doppler spectra of both the single point scatterer and random point scatterers moving in a vessel of diameter of 11 mm were simulated (Fig. 1). The motion of each point scatterer was given by (11). The single point scatterer was assumed to move along the central axis of the vessel at a velocity of 15 cm/s and the random scatterers were assumed to fill up the entire vessel having a velocity profile of either a constant (plug flow at 15 cm/s) or a parabolic function (parabolic flow with a maximum velocity of 30 cm/s),

$$v(r) = v_{max}\left(1 - \frac{r^2}{a^2}\right),\ r \le a, \tag{22}$$

where v_{max} is the maximum velocity, a is the radius of the vessel, and r is the radial distance from the vessel axis. The distance between the transducer and the center of the vessel was 30 mm (z_0 in Fig. 1) and the angle between the velocity and the beam axis (z-axis) was α. 2.25 MHz, 15–cycle and 4–cycle tone bursts were used for the single point scatterer and multiple random scatterers, respectively. To obtain Doppler spectra, 256 A-lines were produced at a pulse repetition rate of 2048 Hz and digitized at 20 MHz. These A-lines were Fourier transformed at different delay times (the time relative to the transmit tone-bursts) to produce velocity profiles along the axial axis of the array beam (Fig. 1). Notice that (13) was not used directly to produce Doppler spectra.

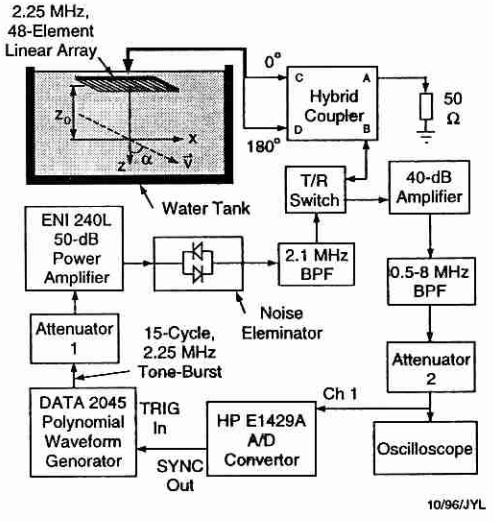

Fig. 2 Block diagram of the experiment for the measurement of velocity vectors of a point scatterer with a limited diffraction layered array beam.

To verify the theory, an experiment for a single point scatterer moving along the axis of an imagined vessel

was performed (Fig. 1). The transducer parameters and the signal processing procedure were exactly the same as those described in the simulation. A block diagram for data acquisition is shown in Fig. 2 where the transducer was weighted with a stepwise [13] sine function of the parameter, k_x = 1649.13 m^{-1} (see Eq. (9)), in the x direction. This weighting was achieved by connecting electronically every 5 adjacent elements of the array together except at each end of the array where 4 elements were connected and by driving the groups of the connected elements with a 15–cycle tone-burst of alternating phase through a hybrid coupler (MACOM 9452). The tone-bursts were produced with a Polynomial Waveform Generator (DATA 2045) and sent to the transducer via an attenuator, 50-dB power amplifier (ENI 240L), noise eliminator, band-pass filter, T/R switch, and the hybrid coupler. Echoes returned from the point scatterer were amplified and digitized at 12–bit resolution and at 20 MHz sampling frequency with an HP E1429A A/D convertor. The system was synchronized by the SYNC signal from the digitizer which triggered both the function generator and the delay unit inside the digitizer. The synchronization removed jittering between A-lines.

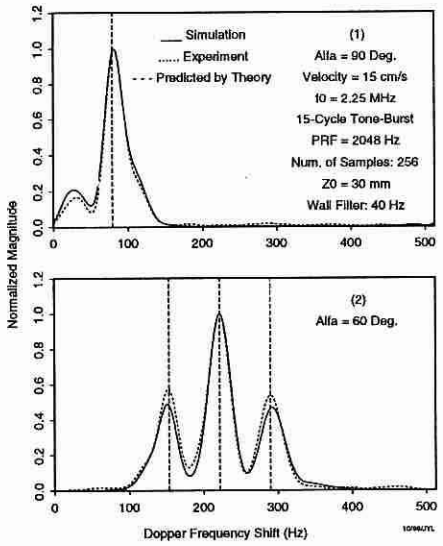

Fig. 3 Doppler spectra of a moving point scatterer centered at the axial distance of 30 mm. The velocity of the scatterer was 15 cm/s with the Doppler angles α or $\pi - \alpha = 90°$ (Panel (1)) and 60° (Panel (2)) (see Fig. 1), respectively. Solid, dotted, and dashed lines represent results from the simulation, experiment, and the prediction from theory, respectively. A wall filter with a cutoff frequency of 40 Hz was used to remove DC (direct current) components.

The Doppler spectra for the simulation and experiment of a single point scatterer moving at 15 cm/s with α or $\pi - \alpha = 90°$ and 60° are shown in Fig. 3(1) and 3(2), respectively. It is seen that there are peaks at the boundaries of the spectra and the experiment, simulation, and theory agree very well with each other. The simulated Doppler spectra of moving random scatterers in a vessel are shown in Fig. 4 where both plug and parabolic flows are assumed. In Fig. 4, we also see a good agreement between the theoretical prediction and the simulation except that for the parabolic flow, the maximum velocity appears smaller in the simulation. This is because the transducer is not focused in the elevation direction and thus multiple velocities are presented simultaneously in a large resolution cell.

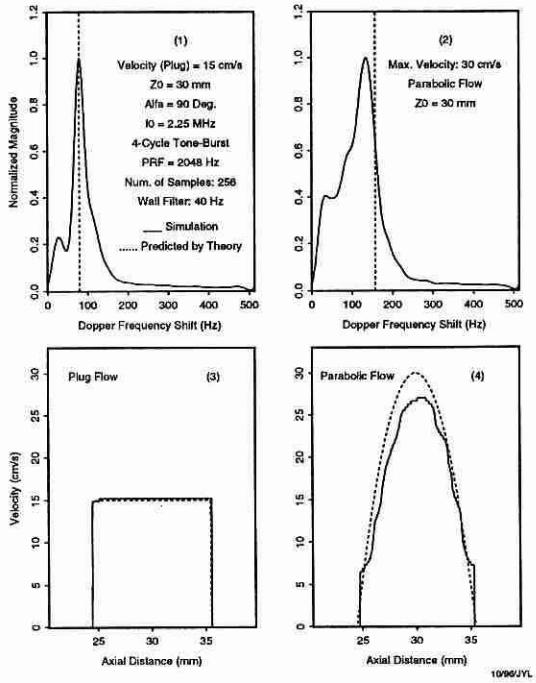

Fig. 4 Doppler spectra and velocity profiles of moving random point scatterers in a vessel of a diameter of 11 mm centered at an axial distance of 30 mm with the Doppler angle of 90° (transverse flow). Results of both plug (Panels in the left column) and parabolic (Panels in the right column) flows are shown. Panels in the top row are spectra at the depth of 30 mm and the panels in the bottom row are velocity profiles corresponding to those in the top row. 20 independent spectra were averaged to obtain the results. Solid and dotted lines indicate the simulation results and the theoretical predictions, respectively. A wall filter with a cutoff frequency of 40 Hz was applied.

IV. DISCUSSION

From the results in Figs. 3 and 4, it is seen that the Doppler spectra obtained with limited diffraction layered

array beams [6–8] have peaks at the boundaries in addition to the central peak. The peaks at the boundaries are related to the transverse velocity of flow (19) and the central peak indicates the regular Doppler frequency shift (18). From these two components of a velocity, the velocity vector can be calculated ((20) and (21)). In addition, because layered array beams can be implemented with a linear array and the weighting for the array is simple (stepwise sine or cosine weighting), this method can be easily incorporated into commercial scanners for measuring transverse velocity of flow. If the array is focused in the elevation (y) direction, the accuracy of the measurement will be improved for the transverse flow. It should be noticed that the elevation focusing will not affect the beam profiles in the perpendicular direction (Fig. 5). This means that the method developed above is also applicable to the case of elevation focusing with an advantage that the slice thickness at the focus is reduced and a disadvantage that the beams are no longer limited diffraction and thus may have a short depth of field, especially, for a small f-number.

Because layered array beams do not focus in the x direction, the beamwidth may be as wide as the array aperture in this direction (about 18.288 mm in this paper). If there exist multiple velocities simultaneously within this aperture, the peaks of the Doppler spectra may be broadened or disappear. Therefore, the method developed in this paper is most suitable for transverse flow measurement where the conventional Doppler method fails, such as the flow in carotid arteries, where the x-axis of the array is in parallel with the axis of the flow. To ensure the transducer surface is in parallel with flow, conventional imaging can be used to first align the transducer before the velocity measurement. However, as the frequency of the array beams is increased, the size of transducer and thus the size of resolution cell can be reduced in both directions of the array without reducing the depth of field [6,14].

In addition, with the array beams derived in (7), the relationship between the temporal Fourier transform of the echo signal and the spatial Fourier transform of the object function can be established [11–12]. This allows the construction of the object function in a very high resolution and low sidelobes without reducing image frame rate (two-way dynamic focusing) [12–12]. Because Fast Fourier transform can be used, the hardware implementation of the imaging method will be much simpler than the conventional digital dynamic focusing systems. If a plane wave is used in transmission (set both $k_x = 0$ and $k_y = 0$) and limited diffraction array beams of different k_x and k_y are used in reception, the imaging system can construct either 2D or 3D images at a very high frame rate up to 3750 frames/s for a depth of 200 mm in biological soft tissues [11–12].

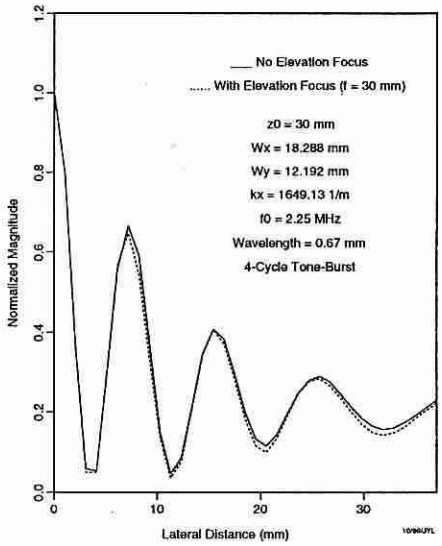

Fig. 5 Simulated lateral profiles of limited diffraction array beams (plotted along the x-axis from the center of the linear array shown in Fig. 1) at an axial distance of 30 mm with (dotted line, focal length is 30 mm) and without (solid line) focusing in the elevation (y) direction. 4–cycle, 2.25 MHz tone burst was assumed. The weighting function in the x-direction was given by $\cos k_x x$ where $k_x = 1649.13$ m^{-1}.

V. CONCLUSION

New limited diffraction beams called array beams [6–8] are used to measure velocity vector of flow. Results show that Doppler spectra obtained with these beams have peaks at the boundaries of the spectra which may improve the accuracy of the measurement of the transverse velocity. This is particular useful for measuring blood flows in some vessels, such as, carotid arteries, that run in parallel with skin without using a wedge stand. The new beams can be produced with a linear array and easily incorporated into commercial scanners. In addition, the array beams can be used for high frame rate imaging (up to 3750 frames/s for a depth of 200 mm in biological soft tissues) or to achieve dynamic focusing in both transmit and receive without reducing frame rate with relatively simple and inexpensive hardware than conventional digital beam formers [11–12].

Acknowledgment — This work was supported in part by grants CA54212 and CA43920 from the National Institutes of Health. The author thanks the preparation of the experiment by Randy R. Kinnick in the Ultrasound Laboratory at the Mayo Clinic.

VI. REFERENCES

1. J. A. Stratton, *Electromagnetic Theory.* New York and London: McGraw-Hill Book Company, 1941, Page 356.
2. J. Durnin, J. J. Miceli, Jr., and J. H. Eberly, "Diffraction-free beams," *Phys. Rev. Lett.*, vol. 58, no. 15, pp. 1499–1501, April 13, 1987.
3. G. Indebetow, "Nondiffracting optical fields: some remarks on their analysis and synthesis," *J. Opt. Soc. Am. A*, vol. 6, no. 1, pp. 150–152, Jan., 1989.
4. D. K. Hsu, F. J. Margetan, and D. O. Thompson, "Bessel beam ultrasonic transducer: fabrication method and experimental results," *Appl. Phys. Lett.*, vol. 55, no. 20, pp. 2066–2068, Nov. 13, 1989.
5. J. A. Campbell and S. Soloway, "Generation of a nondiffracting beam with frequency independent beam width," *J. Acoust. Soc. Am.*, vol. 88, no. 5, pp. 2467–2477, Nov., 1990.
6. Jian-yu Lu, "Limited diffraction array beams," *International Journal of Imaging System and Technology* (to appear in January, 1997).
7. Jian-yu Lu, "Designing limited diffraction beams," *IEEE Trans. Ultrason. Ferroelec. Freq. Contrl.* (to appear in January, 1997).
8. Jian-yu Lu, "Construction of limited diffraction beams with Bessel bases," in *IEEE 1995 Ultrasonics Symposium Proceedings,* 95CH35844, vol. 2, pp. 1393–1397, 1995.
9. Jian-yu Lu, "Bowtie limited diffraction beams for low-sidelobe and large depth of field imaging," *IEEE Trans. Ultrason. Ferroelec. Freq. Contrl.*, vol. 42, no. 6, pp. 1050–1063, November, 1995.
10. Jian-yu Lu, "Producing bowtie limited diffraction beams with synthetic array experiment," *IEEE Trans. Ultrason. Ferroelec. Freq. Contrl.* vol. 43, no. 5, pp. 893–900, September, 1996.
11. Jian-yu Lu, "2D and 3D high frame rate imaging with limited diffraction beams," *IEEE Trans. Ultrason. Ferroelec. Freq. Contrl.* (submitted).
12. Jian-yu Lu, "Experimental study of high frame rate imaging with limited diffraction beams," *IEEE Trans. Ultrason. Ferroelec. Freq. Contrl.* (submitted).
13. Jian-yu Lu and J. F. Greenleaf, "Ultrasonic nondiffracting transducer for medical imaging," *IEEE Trans. Ultrason. Ferroelec. and Freq. Contr.*, vol. 37, no. 5, pp. 438–447, Sept., 1990.
14. Jian-yu Lu and J. F. Greenleaf, "Nondiffracting X waves — exact solutions to free-space scalar wave equation and their finite aperture realizations," *IEEE Trans. Ultrason. Ferroelec. and Freq. Contr.*, vol. 39, no. 1, pp. 19–31, Jan., 1992.
15. Jian-yu Lu and J. F. Greenleaf, "Experimental verification of nondiffracting X waves," *IEEE Trans. Ultrason. Ferroelec. and Freq. Contr.*, vol. 39, no. 3, pp. 441–446, May, 1992.
16. Jian-yu Lu, He-hong Zou, and J. F. Greenleaf, "Biomedical ultrasound beam forming," *Ultrasound Med. Biol.*, vol. 20, no. 5, pp. 403–428, July, 1994.
17. Jian-yu Lu, Tai K. Song, Randall R. Kinnick, and J. F. Greenleaf, "*In vitro* and *in vivo* real-time imaging with ultrasonic limited diffraction beams," *IEEE Trans. Med. Imag.*, vol. 12, no. 4, pp. 819–829, Dec., 1993.
18. Jian-yu Lu and J. F. Greenleaf, "Diffraction-limited beams and their applications for ultrasonic imaging and tissue characterization," in *New Developments in Ultrasonic Transducers and Transducer Systems,* F. L. Lizzi, Editor, Proceedings of SPIE, vol. 1733, pp. 92–119, 1992.
19. Jian-yu Lu and J. F. Greenleaf, "Application of Bessel beam for Doppler velocity estimation," *IEEE Trans. Ultrason. Ferroelec. and Freq. Contr.*, vol. 42, no. 4, pp. 649–662, Jul., 1995.
20. J. N. Brittingham, "Focus wave modes in homogeneous Maxwell's equations: transverse electric mode," *J. Appl. Phys.*, vol 54, no. 3, pp. 1179–1189, 1983.
21. R. W. Ziolkowski, "Exact solutions of the wave equation with complex source locations," *J. Math. Phys.*, vol. 26, no. 4, pp. 861–863, April, 1985.
22. V. L. Newhouse, E. S. Furgason, G. F. Johnson, and D. A. Wolf, "The dependence of ultrasound Doppler bandwidth on beam geometry," *IEEE Trans. Sonic. Ultrason.*, vol. SU-27, pp. 50–59, 1980.
23. I. A. Hein, "3–D blood flow velocity estimation with a triple-beam lens — experimental results," in *IEEE 1995 Ultrasonics Symposium Proceedings,* 95CH35844, vol. 2, pp. 1471–1476, 1995.
24. D. Vilkomerson, D. Lyons, and T. Chilipka, "Diffractive transducers for angle-independent velocity measurements," in *IEEE 1994 Ultrasonics Symposium Proceedings,* 94CH3468–6, vol. 3, pp. 1677–1682, 1994.
25. Y. M. Kadah and A. H. Tewfik, "Efficient design of ultrasound true-velocity flow mapping," *Engineering in Medicine and Biology* (submitted).
26. N. T. Sanghvi, R. Shinomura, C. Nakaya, and K. Katakura, "Frequency scanning, front viewing, alternating polarity transducer array for ultrasound imaging system," in *New Developments in Ultrasonic Transducers and Transducer Systems,* F. L. Lizzi, Editor, Proceedings of SPIE, vol. 260, pp. 260–263, 1992.